7388 *Macromolecules* **2009**, *42*, 7388–7395
DOI: 10.1021/ma9012253

Macromolecules
ARTICLE

Multiblock Copolymers of Lactic Acid and Ethylene Glycol Containing Periodic Side-Chain Carboxyl Groups: Synthesis, Characterization, and Nanoparticle Preparation

Dhawal D. Ankola,[†] M. N. V. Ravi Kumar,[†] Federica Chiellini,[‡] and Roberto Solaro*,[‡]

[†]*Strathclyde Institute of Pharmacy and Biomedical Sciences, University of Strathclyde, 27 Taylor Street, Glasgow G4 0NR, U.K, and* [‡]*Department of Chemistry and Industrial Chemistry, University of Pisa, via Risorgimento 35, 56126 Pisa, Italy*

Received June 8, 2009; Revised Manuscript Received July 24, 2009

ABSTRACT: Multiblock copolymers containing periodically spaced side-chain carboxyl groups were obtained by a two-step synthesis involving the preparation of ABA triblock prepolymers of lactic acid (A block) and ethylene glycol (B block) followed by chain extension to $(ABA)_n$ multiblock copolymers by reaction with pyromellitic dianhydride (PMDA). A series of polymer grades were synthesized by varying PEG and PLA chain length. NMR analysis demonstrated the incorporation of PMDA in polymer chain and revealed the possibility of PMDA units to exist in two isomers, *cisoid* and *transoid* forms. Chain extension resulted in the incorporation of free carboxylic groups in polymer backbone and in a 6-fold increase of molecular weight. Thermal analysis indicated that the extended polymers are more stable and have a T_g of 30−50 °C higher than their prepolymers. The polymers were found to be fast degrading in water following coupled first-order kinetics. Further, the carboxylated polymers can be processed into nanoparticulates by either nanoprecipitation or emulsion−diffusion methods resulting in 50−200 nm sized particles.

Introduction

In the recent past, the synthesis of new biodegradable polymers has attained significant interest to fulfill the unmet needs in healthcare. Several families of polymers like polyesters, polyurethanes, polyanhydrides, polyamides, poly(amino acids), and polyorthoesters have found interesting applications catering medical needs.[1−3] Over the years the focus has shifted toward designing and synthesizing biodegradable polymers with tailored properties for specific applications by several approaches which include developing novel synthetic polymers with unique chemistry to increase the diversity of polymer structure, establishing biosynthetic processes to form stimuli-sensitive polymer structures, and adopting combinatorial and computational approaches in biomaterial design.[4−6]

Polymers have found many applications in drug delivery because of their ability to control and to sustain drug release, thus providing an opportunity for improving the potential and reliability of drugs. In particular, polyesters such as polylactide (PLA), polyglycolide (PGA), and their copolymer poly(lactide-*co*-glycolide) (PLGA) have been extensively used for drug delivery applications because of their superior biocompatibility and biodegradability.[1,3] Over the years many investigations have attempted to functionalize polyesters to improve their ability to entrap different molecules and to modify drug release. The hydrophilicity of polyester was enhanced by introducing poly(ethylene glycol) (PEG) segments.[7,8] These amphiphilic block copolymers attracted a great deal of attention because of their ability to form various types of particles for drug delivery and become an important tool in the delivery of chemotherapeutic agents.[9] Many investigators have also tried to enhance the applicability of polyesters by incorporating functional groups into polymer backbone. Many different copolymers of polyesters with different pendant reactive moieties such as hydroxyl,[10,11] carboxyl,[12−14] and amino[15] groups have been synthesized. However, their preparation often involved many synthetic steps in order to modify the physical−chemical properties of the polymer chain.[12,16]

Carboxylated polymers provide several advantages in designing delivery systems due to versatile nature of carboxyl groups. The carboxyl groups have been explored for various applications from enhancing protein entrapment in a nanoparticulate system[17] to utilizing their reactivity for polymer drug conjugation.[18] Carboxyl-functionalized PLGA-*b*-PEG copolymer was synthesized by direct conjugation of PLGA-COOH with NH_2-PEG-COOH to generate PLGA-*b*-PEG-COOH.[19] The negatively ionizable carboxyl functional group also increased the calcification properties of biomaterials.[20] More recently, the ability of particles exposing carboxyl groups to adhere to live malignant cells was reported.[21]

In spite of the several advantages of functional polymers, modifications have been confined mostly to polymer chain end groups because of their synthetic simplicity. The present investigation was aimed at the synthesis, characterization, and processing into nanoparticulates of multiblock copolymers of lactic acid and ethylene glycol containing periodically spaced side-chain carboxyl groups. These new materials might join PLA biodegradability[22] and PEG antiopsonizing properties[23] with the reactivity and bioadhesive properties[24] of carboxyl groups.

Experimental Section

Materials. Toluene (Carlo Erba) was refluxed for 8 h over Na−K alloy under a dry nitrogen atmosphere and then distilled, collecting the fraction having bp 110 °C. Triethylamine (Aldrich) was refluxed for 4 h over CaH_2 under a dry nitrogen atmosphere and then distilled collecting the fraction having bp

*Corresponding author. E-mail: rosola@dcci.unipi.it.

 Published on Web 08/31/2009

89−90 °C. All other solvents were used as received. Poly(ethylene glycol) having average number molecular weight 400 (PEG400, Aldrich) and 1000 Da (PEG1000, Aldrich) were dried by azeotropic distillation with anhydrous toluene under a dry nitrogen atmosphere and used immediately. Stannous(II) octoate ($SnOct_2$, Aldrich), D-α-tocopheryl poly(ethylene glycol) 1000 succinate (TPGS, Eastman Chemical), L-lactide, and D,L-lactide (Aldrich) were used as received.

Dulbecco's Modified Eagles Medium (DMEM), 0.01 M pH 7.4 phosphate buffer saline without Ca^{2+} and Mg^{2+} (PBS_1), calf serum (CS), trypsin/EDTA, glutamine, and antibiotics (penicillin/streptomycin) were purchased from GIBCO Brl. Cell proliferation reagent WST-1 was purchased from Roche Diagnostic. Tissue culture grade disposable plastics were obtained from Corning Costar. Cell lines BALB/3T3 Clone A31 mouse embryo fibroblasts (CCL163) were obtained from American type Culture Collection (ATCC) and propagated as indicated by the supplier.

Prepolymer Synthesis. Lactide−ethylene glycol−lactide triblock copolymers were prepared by a general procedure. Data relevant to the different experiments are reported in Table 1 whereas run pL14 is described in some detail by following. A solution of D,L-lactide (10 g, 70 mmol), dried PEG400 (2.0 g, 5.0 mmol), and 0.1% (w/w) stannous octoate (10 μL, 30 μmol) in 20 mL of dry toluene was heated at reflux for 24 h under a dry nitrogen atmosphere. A small sample (0.25 mL) was withdrawn from the reaction mixture, dried under vacuum, and characterized by NMR and size exclusion chromatography (SEC) analysis. NMR analysis indicated that lactide conversion was 98%. The polymer solution was directly used for chain extension.

Chain Extension. Chain extension of lactide−ethylene glycol−lactide triblock copolymers was performed according to a general procedure. Data relevant to the different experiments are reported in Table 2 whereas run EL14 is described in some detail by the following.

Triethylamine (1.4 mL, 10 mmol) and pyromellitic dianhydride (1.1 g, 5.0 mmol; 1:2:1 copolymer:amine:dianhydride molar ratio) were introduced into the flask containing the pL14 polymer solution under a dry nitrogen atmosphere. The mixture was heated at 110 °C for 1 h under stirring, and then toluene was removed under vacuum. The dried polymer was dissolved in dichloromethane, washed with cold 0.5 N HCl and water in that order, and then precipitated from dichloromethane solution into diethyl ether. The precipitate was collected by filtration and dried under vacuum to yield 10.8 g (82%) of colorless polymeric product. The polymer was further purified by precipitation from acetone in 5% $NaHCO_3$, washing with water, and dried under vacuum.

Preparation of Nanoparticles by Nanoprecipitation. The polymer (25 mg) was dissolved in 5 mL of acetone by stirring at 1000 rpm for 30 min. The resulting solution was then added dropwise by a syringe to 20 mL of water under magnetic stirring at 1000 rpm. The preparation was left under stirring for 6 h, leading to complete evaporation of acetone. The particle size, size distribution, and zeta potential were measured immediately after suspension preparation.

Preparation of Nanoparticles by the Emulsion−Diffusion Method. Nanoparticles were prepared by a slight modification of the emulsion−diffusion−evaporation method.[25] The polymer (25 mg) was dissolved in 1.25 mL of dichloromethane under stirring for 30 min at 1000 rpm. The resulting solution was then added dropwise to an aqueous phase (2.5 mL) containing 5% w/v of stabilizer. The dispersion was kept under stirring for 1 h followed by homogenization (Polytron PT4000; Polytron Kinematica, Switzerland) to reduce droplet size. The emulsion was then diluted with water to a large volume to effect solvent diffusion, resulting into nanoprecipitation. *N*,*N*-Didodecyl-*N*,*N*-dimethylammonium bromide (DMAB), poly(vinyl alcohol) (PVA), and TPGS were screened as stabilizers. Particle size, size distribution, and zeta potential were measured immediately after suspension preparation.

Table 1. Preparation of ABA-Type PLA−PEG−PLA Block Copolymers

	PEG diol		lactide			polymer			
run[a]	M_n	(mmol)	type	(mmol)	conv (%)	M_n[b]	M_n[c]	M_n[d]	PDI[d]
pDL54	400	10	D, L	70	>98	1400	1430	1150	1.24
pL54	400	10	L	70	>98	1400	1470	1220	1.30
pL51	1000	10	L	70	>98	2000	2100	1900	1.23
pL14	400	10	L	140	>98	2400	2990	3210	1.21

[a] In the presence of 0.1% (w/w) of $SnOct_2$, for 24 h at reflux. [b] Computed from the feed composition. [c] By NMR. [d] By SEC.

Table 2. Preparation of Carboxylated Chain-Extended $(ABA)_n$ Polymers by Reaction of Prepolymers with Pyromellitic Dianhydride (PMDA) in the Presence of Triethylamine (TEA) and/or Stannous Octoate ($SnOct_2$)

	prepolymer					polymer	
run[a]	sample	M_n[b]	PDI[b]	catalyst	yield (%)	M_n[b]	PDI[b]
E54T	pDL54	1150	1.24	TEA	47	4900	2.32
E54S	pDL54	1150	1.24	$SnOct_2$	36	1900	1.84
EDL54	pDL54	1150	1.24	TEA/$SnOct_2$	71	8700	2.02
EL54	pL54	1220	1.30	TEA/$SnOct_2$	76	7500	2.16
EL51	pL51	1900	1.23	TEA/$SnOct_2$	67	12800	3.21
EL14	pL14	3210	1.21	TEA/$SnOct_2$	82	16300	3.01

[a] At 110 °C for 1 h; polymer/PMDA molar ratio = 1; TEA/PMDA molar ratio = 2; $SnOct_2$ 0.1% (w/w). [b] By SEC.

Investigation of the Effect of pH on Size and Zeta Potential of Nanoparticles. The pH of nanoparticle suspension (5 mL) was adjusted to 1 by addition of 1 N HCl, and then the suspension was titrated to pH 7.5 with 0.1 N NaOH. Particle size and zeta potential was measured at 1 ± 0.5 pH increments at 25 °C.

***In Vitro* Degradation.** The *in vitro* degradation behavior of polymers was studied in phosphate buffers saline (PBS), pH 7.4 at 37 °C in test tubes.[26] 150 mg of polymer powder (50−100 mesh, 0.3−0.15 mm) was dispersed in 10 mL of PBS into test tubes that were vortexed for 20 min. At fixed time intervals the test tubes were vortexed for 10 min; 200 μL of samples were withdrawn, vacuum-dried, and analyzed by SEC.

***In Vitro* Cytotoxicity.** Tests were performed according to ISO 10993-5 specifications.[27] The powdered (20−40 mesh, 0.9−0.4 mm) polymer sample (EL14) was immersed at a concentration of 0.2 g/mL in DMEM supplemented with 10% calf serum, 4 mM L-glutamine, and 100 U/mL:100 μg/mL penicillin:streptomycin for 48 h at 37 °C in an enriched 5% CO_2 atmosphere. The medium containing the polymer extract was tested undiluted and diluted at a volume ratio of 1:1 and 1:4 using the complete culture medium. Balb/c 3T3 Clone A31 cells were seeded at a density of 1×10^3/well in a 96-well plate and allowed to proliferate for 24 h. The culture media was then changed with the DMEM containing the polymer extracts, and cells were allowed to proliferate for further 24 h at 37 °C in 5% CO_2 enriched atmosphere. Cells incubated with complete DMEM were used as negative controls, and wells containing only complete DMEM were used as blank. At the end of the exposure time, cell viability was measured using WST-1 tetrazolium salt.[28,29] Absorbance of formazan was measured at 450 nm, and values relative to control were reported. All experiments were performed in triplicates.

Measurements. *Size Exclusion Chromatography* (*SEC*). Analyses were performed in chloroform by using a Jasco PU-1580 HPLC pump equipped with two 300 × 7.5 mm PL Mixed-D columns, Jasco 830-RI refractive index detector, and Perkin-Elmer LC-75 spectrophotometric detector. Monodispersed polystyrene samples were used as calibration standards. ^1H NMR spectra were recorded at room temperature in $CDCl_3$ using a Varian Gemini 200 spectrometer and tetramethylsilane (TMS) as internal standard.

Thermal Gravimetric Analysis (*TGA*). Measurements were carried out under a nitrogen atmosphere in the 25−600 °C range at 10 °C/min scanning rate on 10−20 mg polymer samples by a Mettler TG 50 instrument. Onset decomposition temperatures (T_d) were evaluated at 5% weight loss.

Differential Scanning Calorimetry (*DSC*). Analyses were performed on 8−12 mg samples at 10 °C/min scanning rate by a Mettler DSC 30 instrument. Glass transition temperatures were measured at the inflection point of the thermograms relevant to the second heating cycle. Indium and gallium samples were used as calibration standards. In order to promote crystallization, samples were either annealed at 85 °C for 2.5 h or cooled down from 160 at −0.2 °C/min.

Proton Nuclear Magnetic Resonance (*^{1}H NMR*). Spectra were recorded on 5−10% sample solution in perdeuterad solvents by a Varian Gemini 200 spectrometer.

Polarized Optical Microscopy (*POM*). Observations were performed by a Reichert−Jung Polivar microscope equipped with polarizers, digital camera, Mettler FP52 hot plate, and Mettler FP5 temperature controller. Polymer films cast from 10% dichloromethane solution on glass slides were heated to 160 °C and then cooled at −0.2 °C/ min to room temperature and then observed under polarized light.

Atomic Force Microscopy (*AFM*). Samples were imaged in tapping mode with a Multimode Nanoscope IV AFM (Veeco, Santa Barbara, CA) equipped with E-type piezoelectric scanner and NSG01 (NT-MDT Co., Moscow, Russia) cantilevers having 5.5 N/m nominal elastic constant and 150 kHz resonance frequency. Both topography and phase images were collected. Nanoparticle suspensions were centrifuged at 10 000 rpm for 10 min; a small amount of the solid residue was then placed on a mica dish and dried under a dry nitrogen flow. Polymer films were spin-coated on mica dishes from 1% chloroform solutions; before imaging, the films were heated at 160 °C for 5 min and then cooled from 160 to 25 at 0.2 °C/min.

Average Particle Size and Zeta Potential. The mean particle size of the prepared nanoparticle suspensions was measured by dynamic light scattering (Nano ZS, Malvern, UK) taking the average of five measurements, which represented the hydrodynamic diameter of the particles. Mean size was derived from Cumulants analysis of the measured correlation curve, wherein a single particle size is assumed and a single-exponential fit is applied to the autocorrelation function. In addition to the mean particle size, the instrument reports a value (size dispersion index, SDI) included between 0 (monodispersed particles) and 1 (polydispersed particles). The zeta potential was estimated on the basis of electrophoretic mobility under an electric field as an average of 30 measurements. The frequency shift of an incident laser beam caused by these moving particles is converted to the zeta potential by the application of the Smoluchowski equation. The temperature was kept constant at 25 °C during size and zeta potential measurements.

Results and Discussion

Prepolymer Synthesis. Linear ABA three-block copolymers (also referred to as prepolymers in the following sections) were easily prepared by reaction of lactide with PEG diol in the presence of stannous octoate ($SnOct_2$) as catalyst (Table 1).

This catalyst was chosen because of its high efficiency in promoting the ring-opening polymerization of lactide and its approval for biomedical applications by FDA (Food and Drug Administration) due to its low toxicity.[30] Prepolymer samples are named "p" followed by L or DL according to the starting lactide configuration and by two digits indicating the molecular weight of PLA and PEG segments, respectively (4, 5, and 1 correspond to 400, 500, and 1000 Da) computed from the feed compositions. Four different prepolymers were synthesized by varying PLA and PEG chain lengths and by using D,L-lactide and L-lactide. The average molecular weight of three-block copolymers determined by both SEC analysis and NMR characterization generally resulted slightly higher than that computed from the composition of the feed mixture. Very likely, this finding must be attributed to experimental errors. In all cases, the polydispersity index (PDI = M_w/M_n) was in the 1.2−1.3 range.

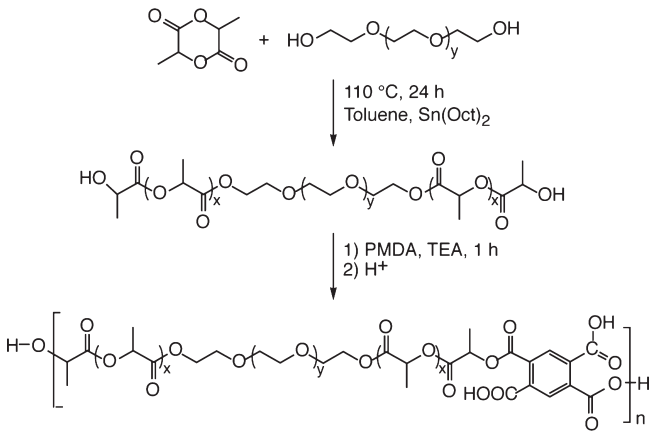

Figure 1. Synthetic procedure adopted for the preparation of multiblock copolymers of lactic acid and ethylene glycol containing periodic side-chain carboxyl groups.

Chain Extension. A few studies have been carried out to convert hydroxyl-terminated triblock copolymers into multiblock copolymers by reaction with diisocyanates and dichlorophosphates.[31,32] However, these techniques do not provide side-chain functional groups. On the other hand, the molecular weight of recycled poly(ethylene terephthalate) can be extended by reaction with pyromellitic dianhydride.[33] By following a similar approach, $(ABA)_n$ polymers containing periodically spaced side-chain carboxyl groups were obtained by chain extension of ABA prepolymers with pyromellitic dianhydride (PMDA) in the presence of triethylamine (TEA) as catalyst (Figure 1). Extended polymer samples are named by replacing the "p" prefix of the corresponding prepolymers with "E". Preliminary experiments indicated that only a limited increase of the molecular weight was achieved in the presence of either TEA (Run E54T) or $SnOct_2$ (Run E54S), whereas a synergic effect was observed when both TEA and $SnOCt_2$ were present in the reaction mixture (Table 2). The dependence of the extent of chain extension on both catalysts can be explained by assuming that lactide polymerization gives the tin alkoxide of the triblock copolymer. Ring-opening of the anhydride then occurs via coordination of the polymeric alkoxide to one of the anhydride carbonyl groups followed by the ring-opening. TEA could help by activating the anhydride bonds and/or by removing the octanoic acid formed by reaction of $SnOct_2$ with reagent moisture. On an average, the molecular weight of the final polymers was about 6−7 times that of the corresponding prepolymer. From the adopted prepolymer/PMDA molar ratio, one could expect much larger polymer molecular weight. On the other hand, errors made in determining the actual prepolymer content and composition in the reaction mixture can easily lead to prepolymer/anhydride ratios different from unity and hence in reduced chain extension.

^{1}H NMR Characterization. The ^{1}H NMR spectra of ABA-type prepolymers in DMSO-d_6 presented peaks at 1.44 and 5.18 ppm attributable to PLA methyl and methyne protons and at 3.48 ppm due to PEG methylenes. The signal at 3.3 ppm was assigned to water moisture in the deuterated solvent. The peaks at 3.58 and 4.18 ppm were attributed to

PEG methylenes linked to hydroxyl end groups and to PLA units (junctions), respectively. In addition to these signals, the ^{1}H NMR spectra of chain-extended polymers presented one peak at 5.35 ppm due to PLA methynes esterified by pyromellitic anhydride (Figure 2). Three further small peaks were detected at 7.9, 8.0, and 8.1 ppm, attributable to aromatic protons of pyromellitic diesters. In particular, the peak at 8.0 ppm was assigned to the more symmetric *transoid* isomer whereas signals at 7.9 and 8.1 ppm were assigned to the *cisoid* isomer that contains two nonequivalent aromatic protons H and H′ (Figure 3). In agreement, the three peaks moved at 8.02, 7.62, and 7.17 ppm when the polymer samples were neutralized with $NaHCO_3$ because of the inductive effect of negatively charged carboxylate groups.

Chemical shift evaluation by additive group contributions confirmed the above assignments. Within the limits of experimental errors, the three aromatic proton peaks have 1:2:1 relative intensity, thus suggesting that there is no significant preference for the formation of the *transoid* isomer with respect to the more crowded *cisoid* one. The integrated intensity of the different signals allowed for determining the polymer composition. In all cases, the PMDA/prepolymer molar ratio resulted close to 0.95. In agreement with SEC analysis, these data indicate that most but not all polymer chains are terminated by one pyromellitic residue. Accordingly, each extended polymer chain contained about 6−7 PMDA molecules, that is, 14−16 free carboxylic groups.

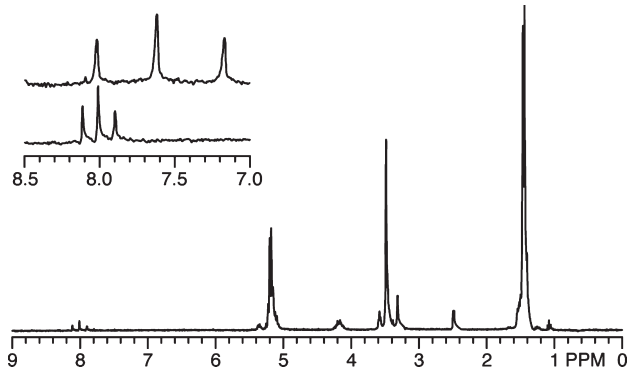

Figure 2. ^{1}H NMR spectrum of EL14 polymer sample in DMSO-d_6. The inset presents the aromatic proton region of the polymer after precipitation in 0.5 N HCl (top) before and in 5% $NaHCO_3$ (bottom).

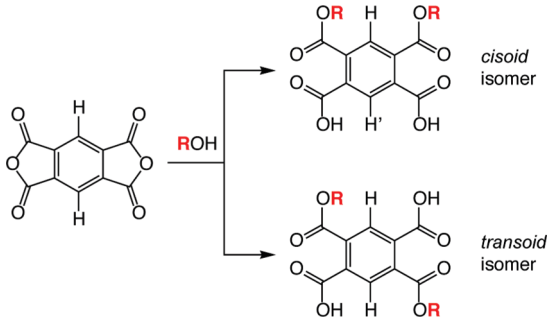

Figure 3. Schematic representation of polymer chain extension by reaction of the prepolymer with pyromellitic dianhydride.

Thermal Analysis. All polymers and prepolymers were characterized by TGA and DSC. TGA curves highlighted the occurrence of two decomposition steps. The temperatures at the onset (T_{on}), at the inflection points of the first and second decomposition step (T_{d1} and T_{d2}), the corresponding weight losses (Δw_1 and Δw_2), and the weight residue at 600 °C (WR_{600}) are summarized in Table 3.

The prepolymers were found to be appreciably less heat stable than the final polymers. Indeed, T_{on}, T_{d1}, and T_{d2} of the extended polymers were about 100, 50, and 10 °C higher than those of the corresponding prepolymers. The weight losses observed for the two decomposition steps closely correspond to the polymer weight content of lactic acid and ethylene glycol units. Moreover, T_{d1} and T_{d2} are in the same range as the decomposition temperatures of PLA and PEG, respectively.[34] Accordingly, these two steps can be attributed mainly to the degradation of PLA and PEG blocks. No decomposition step clearly attributable to the thermal degradation of pyromellitic units was detected very likely because of their rather low content (7−18 wt %) in the polymer and/or peak overlap (T_{dPMDA} = 329 °C).

In all cases, DSC analysis evidenced the presence of only one glass transition in the temperature range between −100 and 160 °C (Figure 4, curve a). On increasing the PLA weight content from 50 to 83%, the T_g of prepolymers and polymers increased from −34.6 to −9.2 °C and from 16.2 to 43.7 °C, respectively (Table 3), in agreement with the larger stiffness and higher T_g (59.1 °C) of PLA blocks.[35]

As indicated, the T_g of the extended polymers was about 30−50 °C higher than that of the corresponding prepolymers because of both the increased molecular weight and the stiffness of the aromatic chain extender. As expected, both the polymer (EDL54) and prepolymer (pDL54) containing racemic PLA blocks did not present any first-order transition attributable to polymer crystallization or melting. The DSC of all other polymer samples also did not display transitions due to polymer crystallization or melting, in spite of the presence of stereoregular L-lactic acid sequences. Such behavior might be attributed to poly(L-lactic acid) (PLLA) block length that is too short and/or to the crystallization rate that is too low to allow for the formation of a crystalline phase under the adopted experimental conditions because of some sort of confinement at the nanometer scale.[36]

Table 3. Thermal Analysis of the Investigated Prepolymers and Polymers

	DSC				TGA[a]				
polymer	PLA block (wt %)	T_g (°C)	ΔC_p (J/g K)	T_{on} (°C)	T_{d1} (°C)	Δw_1 (%)	T_{d2} (°C)	Δw_2 (%)	WR_{600}(%)
pDL54	71	−21.1	0.55	169	303	71	395	28	1
EDL54	71	26.1	0.42	281	347	69	408	28	3
pL54	71	−10.8	0.48	193	295	70	394	28	2
EL54	71	27.2	0.47	279	341	69	410	28	3
pL14	83	16.2	0.28	232	296	80	357	18	2
EL14	83	43.7	0.47	287	344	82	407	16	2
pL51	50	−34.6	0.99	200	296	52	420	44	4
EL51	50	−9.2	0.61	294	340	48	418	49	3

[a] T_{on} is the onset decomposition temperature, evaluated as 5% weight loss; T_{d1} and T_{d2} are the temperatures at the inflection point of the first and second decomposition steps; Δw_1 and Δw_2 are the weight losses of the first and second decomposition steps; WR_{600} is the mass residue at 600 °C.

To support this hypothesis, the sample EL14 containing the longest stereoregular PLLA blocks and the shortest PEG sequences was heated at 160 °C on a hot stage optical microscope and then cooled down at room temperature at 0.2 °C/min. Optical observation of the sample under cross-polarizers clearly highlighted the presence of typical concentric fringed spherulites (Figure 5a). Atomic force microscopy (Figure 5b) showed the presence of overlapping spherulites of about 25 μm diameter and 1700 nm thickness.

A similar pattern was also observed when a cold EL14 sample was annealed at 85 °C for 2.5 h. It has been reported that PLLA and PLLA segments form ring-banded spherulites in miscible blends and block copolymers. The formation of banded spherulites is attributed to the lamellar twisting

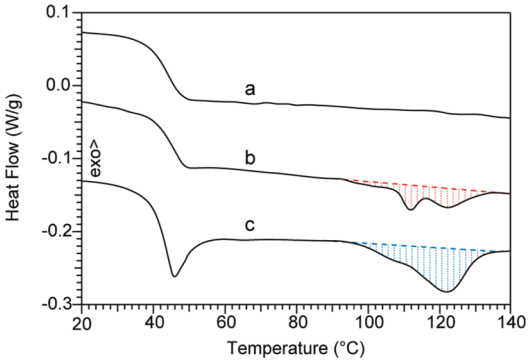

Figure 4. DSC thermograms of EL14 polymer sample: (a) second heating scan after cooling from 160 at 10 °C/min; (b) after annealing at 85 °C; (c) after cooling from 160 to 25 at −0.2 °C/min.

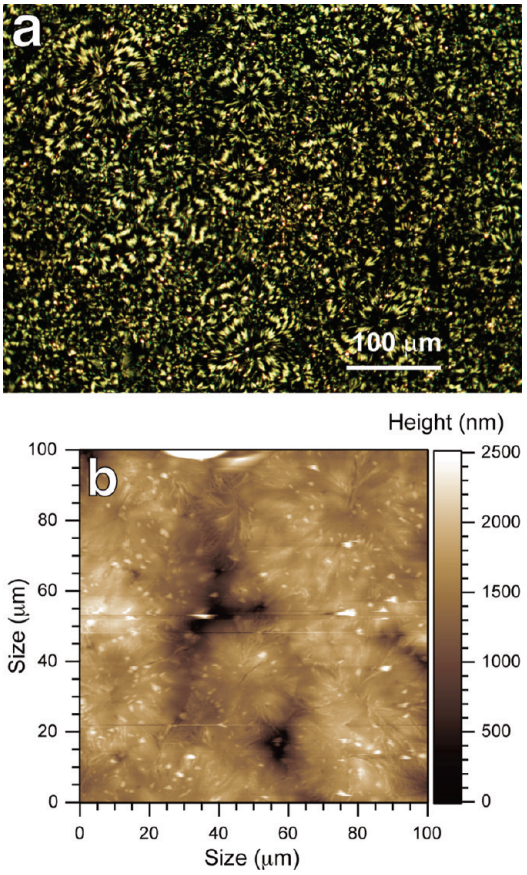

Figure 5. Polarized optical microscopy image (a) and AFM topography (b) of EL14 polymer sample cooled from 160 to 25 at 0.2 °C/min.

along the radial growth direction.[37] It seems therefore reasonable to conclude that the PEG chains are trapped into PLLA spherulites and disturb the regular orientation of crystalline PLLA lamellae.

DSC analysis of the annealed sample showed the occurrence of three overlapping broad melting peaks at 100, 112, and 122 °C with overall ΔH_m = 3.3 J/g (Figure 4, curve b). On the other hand, the slowly cooled sample presented a broad melting peak at 122 °C with a shoulder at about 110 °C having overall ΔH_m = 6.3 J/g (Figure 4, curve c). This result indicates that more regular crystals are formed when the crystallization process occurs at higher temperature. In any case, the recorded ΔH_m values are about 20 and 10 times lower than that of high molecular weight PLLA, whereas the observed melting temperatures are about 40−50 °C lower.[38] We have to stress, however, that none of the other L-lactic acid polymers and prepolymers displayed the presence of a crystalline phase, confirming that the formation of polymer crystals is controlled by both chain length and content of PLLA blocks.

***In Vitro* Degradation.** The *in vitro* degradation of EDL54 and EL54 polymer samples containing D,L-lactic acid and L-lactic acid blocks, respectively, was investigated in pH 7.4 PBS at 37 °C. The polymers were found to degrade rather quickly, the molecular weight of the PEG segment being reached within about 16 days of degradation (Figure 6). The degradation of EL54 and EDL54 followed first-order kinetics with rate constant $k = 5.4 \times 10^{-6}$ and 7.6×10^{-6} s^{-1}, respectively. Unsurprisingly, both polymers have almost the same degradation rate, very likely because the stereoregular EL54 was in an amorphous state.

However, close inspection of SEC traces (Figure 7) shows that most of the molecular weight distributions are made by three overlapping peaks roughly corresponding to the molecular weights of the starting extended polymer, the corresponding prepolymer, and the PEG block.

Apparently, the polymer is initially split into ABA blocks because of the easy hydrolysis of pyromellitic ester bonds. Then, ABA blocks are further split into PLA and PEG segments, in accordance with the easier hydrolysis of the ester bond at PLA−PEG junctions as compared to intra chain PLA ester bonds.[39] Accordingly, the hydrolytic degradation was modeled according to two coupled first-order kinetics having rate constants k_1 and k_2:

$$A \xrightarrow{k_1} B \xrightarrow{k_2} C$$

To verify this hypothesis, each of the SEC curves was decomposed into three Gaussian components, whose relative area was plotted against time (Figure 8) and fitted

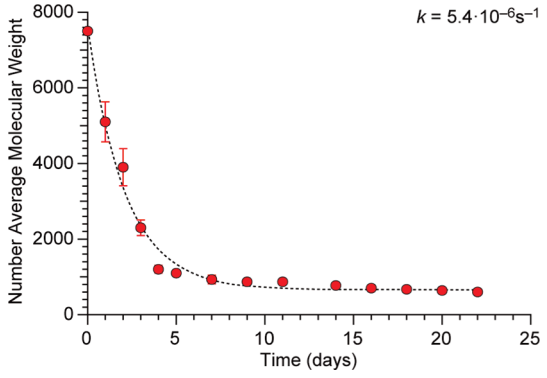

Figure 6. Plot of molecular weight vs time observed during the *in vitro* degradation of EL54. The dashed line represents the best fitting exponential decay.

according to the proposed model. In spite of experimental errors (estimated to be about 10%) and the oversimplified model, the fit is acceptable indicating that the polymer hydrolytic degradation mainly occurs according to the indicated two consecutive steps with similar rate constants k_1 and k_2 of about 2.9×10^{-6} and 2.7×10^{-6} s^{-1} for both EL54 and EDL54.

The reported *in vitro* experiments only demonstrated the polymer hydrolytic degradability. On the other hand, the biodegradability of the resulting polymeric fragments is well documented.[3] Accordingly, the multiblock copolymers could also be claimed biodegradable by extrapolation.

Biological Evaluation. Materials intended for biomedical applications should not release any agent that may be cytotoxic. To investigate whether the extracts of the prepared polymers might be harmful to cells, the fibroblast cell line balb/c 3T3 Clone A31 was cultured in the presence of the extractables of unpurified EL14 for 24 h at 37 °C according to the ISO 10993-5 procedure.[27] WST-1 assay[28,29] was then carried out to evaluate the potential cytotoxicity of the polymer extracts. Aqueous extracts of the investigated sample, undiluted and diluted 1:1 and 1:4, were used. Toxicity tests revealed that the undiluted extract was cytotoxic (no cell growth), although the cytotoxicity showed a significant decrease, with a cell viability of 67 ± 5% and 72 ± 4% after diluting the extract 1:1 and 1:4 with fresh growth medium. However, a cell viability of 54 ± 3% was observed when the same test was repeated on the undiluted extracts of the purified polymer. The observed trend suggests that the investigated polymer sample is not toxic although very careful purification is needed. Indeed, the reported cytotoxicity values are related to polymer extractables, which can contain trace amounts of toxic solvents and catalysts.

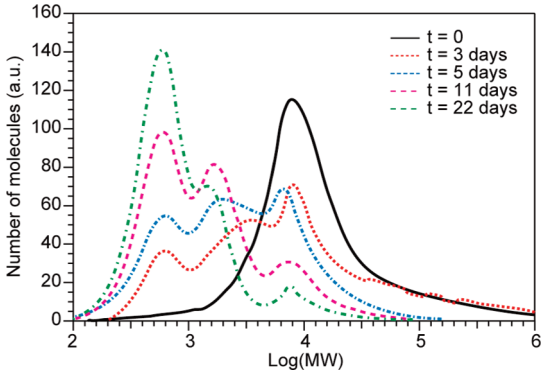

Figure 7. SEC traces recorded at different times during the *in vitro* degradation of EL54.

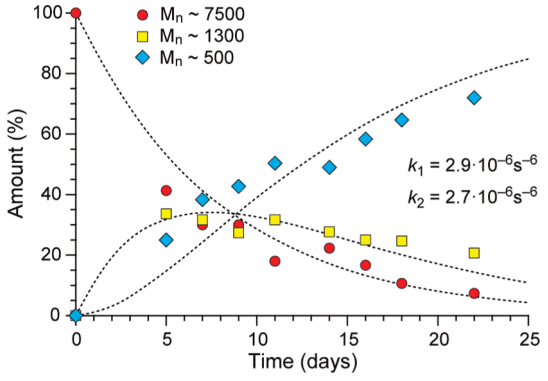

Figure 8. Kinetic plot of individual components of SEC curves recorded at different times during the *in vitro* degradation of EL54.

Nanoparticle Preparation. Nanoparticle suspensions were prepared by both nanoprecipitation[40] and a modified emulsion−diffusion−evaporation[25] method. Indeed, the routine technique being used for formulating PLGA nanoparticles is believed to produce heterogeneous size distribution.[41] The first procedure (also known as solvent displacement method) is better suited for the preparation of nanoparticles loaded with proteic drugs because it does not imply the use of either stabilizers or denaturalizing chlorinated solvents.[42] On the other hand, the emulsion−diffusion method should be preferred when loading lipophilic drugs. Nanoprecipitation was carried out by slowly adding a diluted acetone solution of the polymer into 5-fold excess of water under magnetic stirring. Interestingly, the polymer containing PEG1000 block (EL51) afforded nanoparticles of about 130 nm, whereas the polymers containing PEG400 blocks gave nanoparticles of about 50−60 nm (Table 4). Within the limits of the narrow range of investigated compositions, the reported behavior suggests that in nanoprecipitation the particle size is mostly ruled by the length of hydrophilic PEG blocks and is practically independent of the length of PLA segments. This effect can be tentatively attributed to the extent of polymer swelling in water and hence to the PEG content. It is also possible that the polymer hydrophilicity somehow interferes with the interphase mixing that is responsible for particle formation according to the proposed nanoprecipitation mechanism.[43]

The solid residues obtained by centrifugation of nanoparticle suspensions at 10 000 rpm for 5 min were analyzed by AFM. Topographic images clearly show the presence of spheroidal nanoparticles having a rather narrow size distribution close to that determined by dynamic light scattering (Figure 9). Moreover, a close-up image indicates that the nanoparticle surface is smooth and homogeneous at the nanometer level, thus ruling out that nanoparticles are formed by aggregation of smaller particles.

The slightly elongated shape of nanoparticles could be associated with the shear stress caused by the stirring during nanoparticle preparation and/or high-speed centrifugation. The emulsion−diffusion−evaporation procedure was performed by dropwise addition of the polymer solution in dichloromethane to a 2-fold excess of a water solution containing 5% w/v of stabilizer, followed by homogenization

Table 4. Characteristics of the Prepared Nanoparticles

polymer	preparation method	stabilizer	size[a] (nm)	SDI[a,c]	zeta potential[a,b] (mV)
EL51	nanoprecipitation	none	126 ± 38	0.29 ± 0.08	−44 ± 1
EL14	nanoprecipitation	none	63 ± 5	0.27 ± 0.09	−51 ± 11
EL54	nanoprecipitation	none	53 ± 2	0.19 ± 0.01	−64 ± 10
EDL54	nanoprecipitation	none	56 ± 3	0.26 ± 0.13	−67 ± 9
EL51	emulsion−diffusion	DMAB	46 ± 15	0.32 ± 0.16	52 ± 3
EL51	emulsion−diffusion	PVA	146 ± 19	0.33 ± 0.15	−32 ± 7
EL51	emulsion−diffusion	TPGS	183 ± 26	0.37 ± 0.12	−43 ± 8

[a] All values represented as mean ± standard deviation (n = 3). [b] The zeta potential was measured in the 2.5−3.3 pH range. [c] SDI = particle size dispersion index.

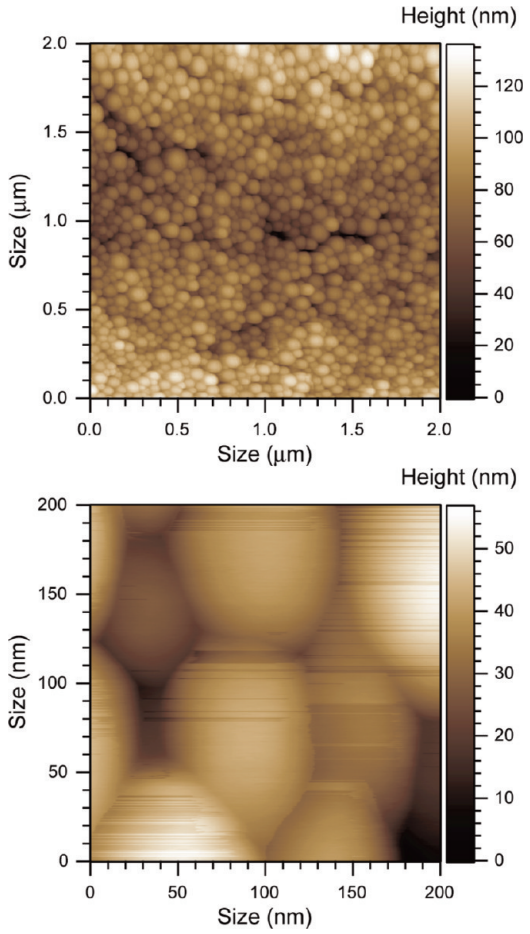

Figure 9. AFM topographic images of the pellet obtained by centrifugation at 10 000 rpm for 5 min of nanoparticles prepared by nanoprecipitation of the EL15 polymer sample.

and dilution with excess water. *N*,*N*-Didodecyl-*N*,*N*-dimethylammonium bromide (DMAB), poly(vinyl alcohol) (PVA), and D-α-tocopheryl poly(ethylene glycol) 1000 succinate (TPGS) were used as stabilizers. DMAB is cationic surfactant that favors emulsion formation whereas PVA is a steric stabilizer that prevents emulsion coalescence by forming a protective film on the surface of emulsion droplets. TPGS is an amphiphilic derivative of vitamin E: the tocopheryl part of the molecule is lipophilic, and the PEG portion is hydrophilic. Thus, despite its bulky shape and large surface area, TPGS acts as a surface-active agent, being miscible in both water and oil.[44] Hydrophobic polymers such as, PLA, PLGA, and PCL can be blended with TPGS, thus forming a matrix material to improve the controlled release of drug from the particles.[44,45]

The type of stabilizer strongly affected the efficiency of the emulsion−diffusion−evaporation method: the nanoparticle size increased from 46 to 146 to 183 nm when using DMAB, PVA, and TPGS as stabilizer under comparable experimental conditions (Table 4). Independent of the preparation method, in all cases the particle size distribution was found to be narrow. The zeta potential was negative for particles prepared using nanoprecipitation method and was in agreement with the presence of carboxylic groups on the particle surface. The zeta potential for particles prepared using DMAB was found to be positive due to the cationic nature of DMAB.

The effect of pH on size and zeta potential was investigated by pH titration of EDL54 nanoparticles prepared by nanoprecipitation (Figure 10). Addition of HCl to bring the suspension to pH 1 caused the particle size to increase from about 60 to 700 nm and the zeta potential from about −70 to +2.5 mV. Increasing the pH by addition of NaOH led to a reduction of particle size and to a sharp decrease of the zeta potential. This phenomenon can be explained by considering that at low pH the carboxyl groups are un-ionized (COOH) with low absolute zeta potential: attenuation of the protective ionic double layer leads to particle aggregation. As the pH increases, the carboxyl groups ionize (COO^-), giving rise to an increase of zeta potential and hence to the electrostatic repulsion of particles leading to smaller nanoparticles. However, the aggregation process is not fully reversible most likely because of adhesion among swollen nanoparticles. In agreement, the particle size decreased from 700 to 200 nm and the zeta potential changed from +2.5 to −17.5 mV as the pH increased from 1 to 5. A further increase of the pH above 5 did not cause any significant change of both particle size and zeta potential. This experiment reveals the possibility of designing particles of varying size as a function of the suspension pH.

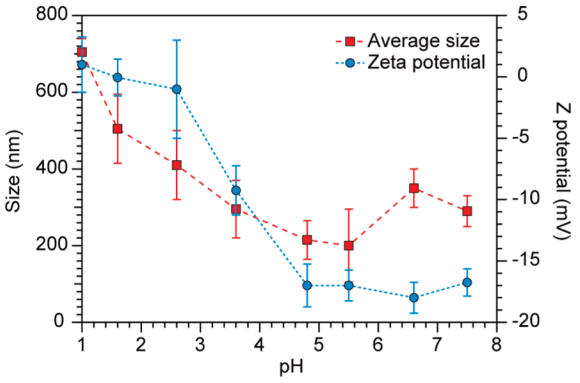

Figure 10. NaOH titration of nanoparticles prepared by nanoprecipitation of EDL54 polymer sample followed by acidification at pH 1 with HCl.

Conclusions

This report illustrates that multiblock copolymers containing periodically spaced side-chain carboxyl groups can be obtained easily by chain extension of lactic acid/ethylene glycol/lactic acid triblock prepolymers with pyromellitic dianhydride (PMDA). Both the hydrophilic/hydrophobic balance of the extended polymer and the periodicity of side-chain carboxyl groups can be modulated by tuning the prepolymer composition and the prepolymer/PMDA molar ratio. Moreover, the extended polymers are hydrolytically degradable and well suited for the preparation of nanoparticle suspensions with narrow size distribution.

Acknowledgment. D.D.A. is thankful to MIUR, Italy, for providing PG fellowship for his one-year stay at Department of Chemistry and Industrial Chemistry, University of Pisa, Pisa, Italy (July 2007−June 2008).

References and Notes

(1) Middleton, J. C.; Tipton, A. J. *Biomaterials* **2000**, *21*, 2335–2346.
(2) Schwendeman, S.; Costantino, H. R.; Gupta, R. K.; Langer, R. In *Controlled Drug Delivery: Challenges and Strategies*; Park, K., Ed.; American Chemical Society: Washington, DC, 1997; pp 229−267.
(3) Domb, A. J., Wiseman, D. M., Eds.; *Handbook of Biodegradable Polymers*; CRC Press: Boca Raton, FL, 1998.
(4) Nair, L. S.; Laurencin, C. T. *Prog. Polym. Sci.* **2007**, *32*, 762–798.
(5) Kim, S.; Kim, J. H.; Jeon, O.; Kwon, I. C.; Park, K. *Eur. J. Pharm. Biopharm.* **2009**, *71*, 420–430.

(6) Bajpai, A. K.; Shukla, S. K.; Bhanu, S.; Kankane, S. *Prog. Polym. Sci.* **2008**, *33*, 1088–1118.
(7) Gref, R.; Minamitake, Y.; Peracchia, M. T.; Trubetskoy, V.; Torchilin, V.; Langer, R. *Science* **1994**, *263*, 1600–1603.
(8) Verrechia, T.; Spenlehauer, G.; Bazile, D. V.; Murry−Brelier, A.; Archimbaud, Y.; Veillard, M. *J. Controlled Release* **1995**, *36*, 49–51.
(9) Ruan, G.; Feng, S. S. *Biomaterials* **2003**, *24*, 5037–5044.
(10) Chiellini, E.; Bemporad, L.; Solaro, R. *J. Bioact. Compat. Polym.* **1994**, *9*, 152–169.
(11) Chiellini, E.; Faggioni, S.; Solaro, R. *J. Bioact. Compat. Polym.* **1990**, *5*, 16–29.
(12) Cerbai, B.; Solaro, R.; Chiellini, E. *J. Polym. Sci., Part A: Polym. Chem.* **2008**, *46*, 2459–2476.
(13) Barrera, D. A.; Zylstra, E.; Lansbury, P. T.; Langer, R. *J. Am. Chem. Soc.* **1993**, *115*, 11010–11021.
(14) Gimenez, S.; Ponsart, S.; Coudane, J.; Vert, M. *J. Bioact. Compat. Polym* **2001**, *16*, 32–37.
(15) Zhao, J.; Quan, D.; Liao, K.; Wu, Q. *Macromol. Biosci.* **2005**, *5*, 636–643.
(16) in't-Veld, P. J. A.; Dijkstra, P. J.; Feijen, J. *Makromol. Chem.* **1992**, *193*, 2713–2730.
(17) Blanco, M. D.; Alonso, M. J. *Eur. J. Pharm. Biopharm.* **1997**, *43*, 287–294.
(18) Khandare, J.; Minko, T. *Prog. Polym. Sci.* **2006**, *31*, 359–397.
(19) Chenga, J.; Teply, B. A.; Sherifi, I.; Sung, J.; Luther, G.; Gu, F. X.; Nissenbaum, E. L.; Moreno, A. F. R.; Langer, R.; Farokhzad, O. C. *Biomaterials* **2007**, *28*, 869–876.
(20) Miyazaki, T.; Ohtsuki, C.; Akioka, Y.; Tanihara, M.; Nakao, J.; Sakaguchi, Y.; Konagaya, S. *J. Mater. Sci.: Mater. Med.* **2003**, *14*, 569–574.
(21) McNamee, C. E.; Y. Aso, Y.; Yamamoto, S.; Fukumori, Y.; Ichikawa, H.; Higashitani, K. *Pharm. Res.* **2007**, *24*, 2370–2380.
(22) Uhrich, K. E.; Cannizzaro, S. M.; Langer, R. S.; Shakesheff, K. M. *Chem. Rev.* **1999**, *99*, 3181–3198.
(23) Gref, R.; Minamitake, Y.; Peracchia, M. T.; Trubetskoy, V.; Torchilin, V.; Langer, R. *Science* **1994**, *263*, 1600–1603.
(24) Park, K.; Robinson, J. R. *Int. J. Pharm.* **1984**, *19*, 107–127.
(25) Hariharan, S.; Bhardwaj, V.; Bala, I.; Sitterberg, J.; Bakowsky, U.; Kumar, M. N. V. R. *Pharm. Res.* **2006**, *23*, 184–189.
(26) D'Souza, S. S.; DeLuca, P. P. *Pharm. Res.* **2006**, *23*, 460–474.
(27) ISO 10993-5: Biological evaluation of medical devices. Part 5: Tests for in vitro cytotoxicity; Geneva, Switzerland, **1999**.
(28) Chiellini, F.; Piras, A. M.; Gazzarri, M.; Bartoli, C.; Ferri, M.; Paolini, L.; Chiellini, E. *Macromol. Biosci.* **2008**, *8*, 516–525.
(29) Piras, A. M.; Chiellini, F.; Fiumi, C.; Bartoli, C.; Chiellini, E.; Fiorentino, B.; Farina, C. *Int. J. Pharm.* **2008**, *357*, 260–271.
(30) Wong, W. H.; Mooney, D. J. In *Synthetic Biodegradable Polymers Scaffolds*; Atala, A., Mooney, A., Eds.; Birkhauser: Boston, 1997; pp 51−82.
(31) Signori, F.; Chiellini, F.; Solaro, R. *Polymer* **2005**, *46*, 9642–9652.
(32) Mao, H.; Kadiyala, I.; Leong, K. W.; Zhao, Z.; Dang, W. In *Encyclopedia of Controlled Drug Delivery*; Mathiowitz, E., Ed.; Wiley-Interscience: New York, 1999; Vol. *1*, pp 45−60.
(33) Awaja, F.; Daver, F.; Kosior, E. *Polym. Eng. Sci.* **2004**, *44*, 1579–1587.
(34) D'Antone, S.; Bignotti, F.; Sartore, L.; D'Amore, A.; Spagnoli, G.; Penco, M. *Polym. Degrad. Stab.* **2001**, *74*, 119–124.
(35) Pan, P.; Zhu, B.; Kai, W.; Dong, T.; Inoue, Y. *Macromolecules* **2008**, *41*, 4296–4304.
(36) Delpouve, N.; Saiter, A.; Mano, J. F.; Dargent, E. *Polymer* **2008**, *49*, 3130–3135.
(37) Xu, J.; Guo, B.-H.; Zhang, Z.-M.; Zhou, J.-J.; Jiang, Y.; Yan, S.; Li, L.; Wu, Q.; Chen, G.-Q.; Schultz, J. M. *Macromolecules* **2004**, *37*, 4118–4123.
(38) Pan, P.; Liang, Z.; Zhu, B.; Dong, T.; Inoue, Y. *Macromolecules* **2009**, *42*, 3374–3380.
(39) Hu, D. S.-G.; Liu, H.-J. *J. Appl. Polym. Sci.* **1994**, *51*, 473–482.
(40) Fessi, H.; Puisieux, F.; Devissaguet, J. P.; Ammoury, N.; Benita, S. *Int. J. Pharm.* **1989**, *55*, R1–R4.
(41) Prabha, S.; Zhou, W-.Z.; Panyam, J.; Labhasetwar, V. *Int. J. Pharm.* **2002**, *244*, 105–115.
(42) Chiellini, E.; Chiellini, E. E.; Chiellini, F.; Solaro, R. *J. Bioact. Compat. Polym.* **2001**, *16*, 441–465.
(43) Davies, J. T.; Rideal, E. K. *Interfacial Phenomena*; Academic Press: New York, 1961.
(44) Mu, L.; Feng, S. S. *J. Controlled Release* **2003**, *86*, 33–48.
(45) Somavarapu, S.; Pandit, S.; Gradassi, G.; Bandera, M.; Ravichandran, E.; Alpar, O. H. *Int. J. Pharm.* **2005**, *298*, 344–347.